Nuclear Instruments and Methods in Physics Research A 755 (2014) 62–68

Contents lists available at ScienceDirect

Nuclear Instruments and Methods in Physics Research A

journal homepage: www.elsevier.com/locate/nima

Testing of triple-GEM chambers for CBM experiment at FAIR using self-triggered readout electronics

A.K. Dubey [a], S. Chattopadhyay [a,*], J. Saini [a], R. Singaraju [a], G.S.N. Murthy [a], Y.P. Viyogi [a], A. Abuhoza [b], S. Biswas [b], U. Frankenfeld [b], J. Hehner [b], V. Kleipa [b], Th. Morhardt [b], C.J. Schmidt [b], D.J. Schmidt [b], A. Lymanets [c,1], H.R. Schmidt [c,1]

[a] Variable Energy Cyclotron Centre, 1/AF Bidhan Nagar, Kolkata 700064, India
[b] GSI Helmholtzzentrum fur Schwerionenforschung GmbH, Darmstadt, Germany
[c] Physikalisches Institut - Eberhard Karls Universitat Tubingen, D-72076 Tubingen, Germany

ARTICLE INFO

Article history:
Received 28 June 2013
Received in revised form
15 March 2014
Accepted 10 April 2014
Available online 21 April 2014

Keywords:
GEM
Self-triggered readout
CBM
Position sensitive particle detectors

ABSTRACT

Triple GEM chamber has been selected to be used for the muon detection system (MUCH) in the Compressed Baryonic Matter (CBM) experiment at the upcoming Facility for the Antiproton and Ion Research (FAIR). Two prototype triple-GEM chambers filled with the mixture of argon and CO_2 gases in the ratio of 70:30 were made of small-size (10 cm × 10 cm) single-mask GEM foils and read by a self-triggered readout ASIC called nXYTER have been tested with pion beams at CERN. The readout electronics records the arrival times of GEM hits and of corresponding coincidence trigger signals separately. The distribution of time difference between GEM hits and respective triggers shows a peak demonstrating the time correlation between GEM hits and the trigger. The width (σ) of the time-correlation peak, which is related to the time resolution of the chamber, reduces with voltage approaching $\approx$12 ns at ΔV_{GEM} of 335 V. Considering the hits inside the time-correlation peak to correspond to the beam trigger, the efficiency reaches a plateau at 95% at Δ_{GEM} above 330 V. For a readout plane segmented by 3 mm × 3 mm pads, on an average 1.2 pads are fired per trigger for pion beams at the operating voltage. The chamber shows a gain of $\approx$4000 at ΔV_{GEM} of 350 V.

1. Introduction

Gas Electron Multiplier (GEM) based detectors have found wide-ranging applications in different fields with a major share in high energy physics experiments [1]. The micro-pattern detectors of this particular type are being used widely mainly due to their reported good time and position resolutions coupled to excellent rate handling capability [2–4]. Even though several large experiments like COMPASS, PHENIX, STAR and end-cap upgrade in CMS have been using GEM-chambers, application-specific R&D needs to be performed for making the detector suitable for any new experiment. The parameters which affect the performance of the detector include inter-electrode distances, applied field, and gas composition apart from the geometry of the GEM foil itself. In this paper, we report the performance of 10 cm × 10 cm single-mask triple-GEM prototypes built for the muon detection system (MUCH) in the proposed Compressed Baryonic Matter (CBM) experiment at the upcoming Facility for Antiproton and Ion Research (FAIR) in Germany.

In the CBM experiment at FAIR [5], as shown schematically in Fig. 1, muons will be detected by six sets of triplets of tracking stations arranged behind six absorbers of varying thicknesses. A set of silicon tracking stations (STS) placed inside a dipole magnet reconstructs the charged tracks. The tracks are then projected outside the magnetic field onto the muon chambers to identify muons. Unlike other conventional muon detection systems in high energy physics experiments, the absorbers in CBM-MUCH are segmented to track muons to a very low transverse momentum.

The CBM experiment aims at exploring the nuclear matter under extreme baryonic density expected to be produced in high energy heavy ion collisions at FAIR. One focus of CBM is to probe the matter with quarkonia states likely to be produced at the early stage of the collisions. Low production cross-section of such states at FAIR energy results in a requirement of unprecedentedly high beam intensity to collect reasonable statistics at a short data taking period. Additionally, the particle multiplicity from the high energy heavy ion collisions at FAIR energy is high. Particles while passing through the absorber segments generate secondaries and the tracking chambers face particles at a rate of 0.3 particles/cm^2.

* Corresponding author.
E-mail address: sub@vecc.gov.in (S. Chattopadhyay).
[1] Also at: High Energy Physics Department, Kiev Institute for Nuclear Research (KINR), Kyiv, Ukraine.

http://dx.doi.org/10.1016/j.nima.2014.04.027
0168-9002/

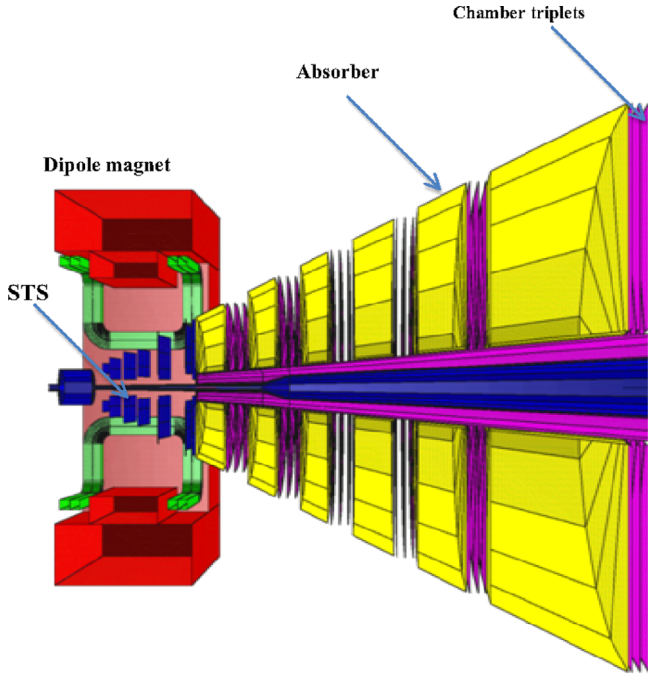

Fig. 1. MUCH setup with six absorbers and six tracking stations. The combination of absorbers and tracking stations is placed downstream of a dipole magnet. Each station consists of three detector layers. First layer is expected to face particle flux of 0.3 particles/cm^2/event at an event rate of 10 MHz. A set of layers, especially in the first three stations, is to be equipped with GEM chambers. A set of silicon stations has been placed inside the dipole magnets for tracking and measurement of charged particle parameters.

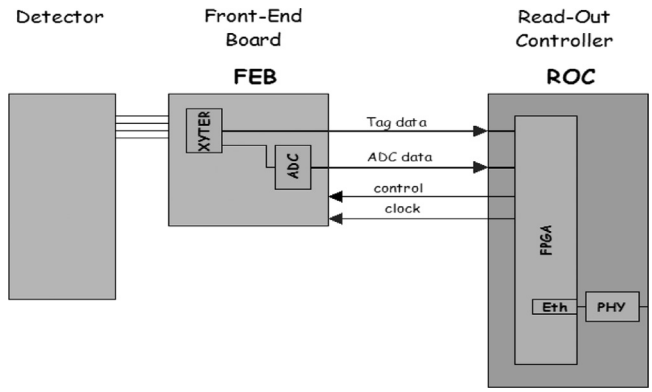

Fig. 2. Schematic of the nXYTER-based readout system. The detector is connected directly to FEB which houses the nXYTER ASIC and ADC. ROC as connected to the FEB is to control the data acquisition.

In such a condition, the most upstream muon chamber will be required to operate at a particle rate of 3 MHz/cm^2. Considering the reported usefulness of the GEM chambers in such an environment, it has been decided to use triple GEM detectors as tracking stations in the first few stations of MUCH. It has been reported earlier that the triple GEM chambers can be operated with $>95\%$ efficiency in pion beam at a rate of 10^5 Hz/mm^2 [6]. The reported spark probability per pion at such an operating voltage is $\approx 10^{-11}$. With the advent of the single-mask GEM technology [7], large size GEM chambers of 50 cm width and 1 m length can now be produced, satisfying the requirement of CBM muon system.

In addition to the above-mentioned detector-specific requirements, operation of CBM-MUCH at a high interaction rate (10 MHz) requires the use of a self-triggered readout electronics. This requirement is guided by the fact that at this high rate of interactions, a good fraction of events are likely to be missed during the time of trigger decision. In the self-triggered readout system, no external event trigger is applied and all hits above a predefined threshold are recorded along with their corresponding arrival times. For testing a detector using such a readout system, signals from the coincidence of the trigger detectors along with their timestamps are also recorded separately. While the time-stamps of the detector hits will be correlated to the time stamp of the corresponding coincidence trigger, the noise hits will not be correlated. For most of the detector tests within CBM, a self-trigger readout system based on a 128-channel ASIC, called nXYTER [8] which was used earlier by the DETNI collaboration, is being used. This ASIC has two independent pulse-processing channels with different peaking times, the fast channel of 30 ns peaking time constant provides the time-stamp of the hit after the discriminator and the slow channel of 140 ns peaking time constant is used for signal amplitude measurement using a peak detection and hold circuit. The ASIC shows a time-jitter smaller than 4 ns for 8×10^3 electron input charge improving to 2 ns at 10^4 electron input. A 12-bit ADC of 25 fC dynamic range is used on the Front End Board (FEB) each of which houses one nXYTER ASIC. The block-diagram of the readout system is shown in Fig. 2, in which the detector is directly connected to the Front End Board. The data transfer and control operations are performed by a Readout Controller (ROC) board. One ROC board can handle at most two FEBs.

As a part of the R&D effort for CBM-MUCH, we have built several triple GEM chambers of varying design parameters. Here we report the testing of two GEM chambers each one built at VECC-Kolkata and at GSI-Darmstadt separately. Both the chambers were made of single-mask GEM foils procured from the CERN PCB lab. However, they differ in readout granularity. The article is organized as follows. We describe in some detail the fabrication procedure of the chambers in Section 2. In Section 3 we describe the test beam setup. Results on gain, efficiency, pad multiplicity are discussed in Section 4. We summarize the results in Section 5 along with future plans.

2. Chamber fabrication

The chamber built at VECC as schematically shown in Fig. 3 and described in Ref. [9] is a gas-tight perspex enclosure, in which different electrodes are arranged at specific gaps using insulating spacers.

The top plane, known as the drift plane, is made of single-sided copper-clad kapton foil affixed on a FR4 frame which was placed as a top lid. Three framed GEM foils each of 10 cm $\times$ 10 cm size, separated by spacers, were placed inside the perspex container. The readout anode plane is made of a PCB, in which the inner side is etched into 512 pads each of 3 mm $\times$ 3 mm size. The pad-dimension of the prototype chamber corresponds to the optimized smallest allowed pad-size in the first GEM station at CBM as obtained by detailed simulation in the CBM framework. The readout plane was a 4-layer PCB, in which traces are guided into four groups each connected to one FEB using two 68-pin connectors fixed to the side of the chamber. Out of the four layers in the readout PCB, one was used exclusively for ground connections. One such chamber, shown in Fig. 4, has been tested at the H4 beam line at CERN in October 2012. The VECC triple GEM chamber tested at CERN had a drift gap of 3 mm, gap between each GEM foil-pair was 1 mm and the gap between the last GEM foil and the readout plane is 1.5 mm. One chamber built using a similar procedure and coupled to the conventional electronics was tested earlier using radioactive sources and cosmic rays as reported in Ref. [9]. In this paper, we present for the first time, the results obtained by using the self-triggered readout system. For all the measurements reported here, the voltages for different

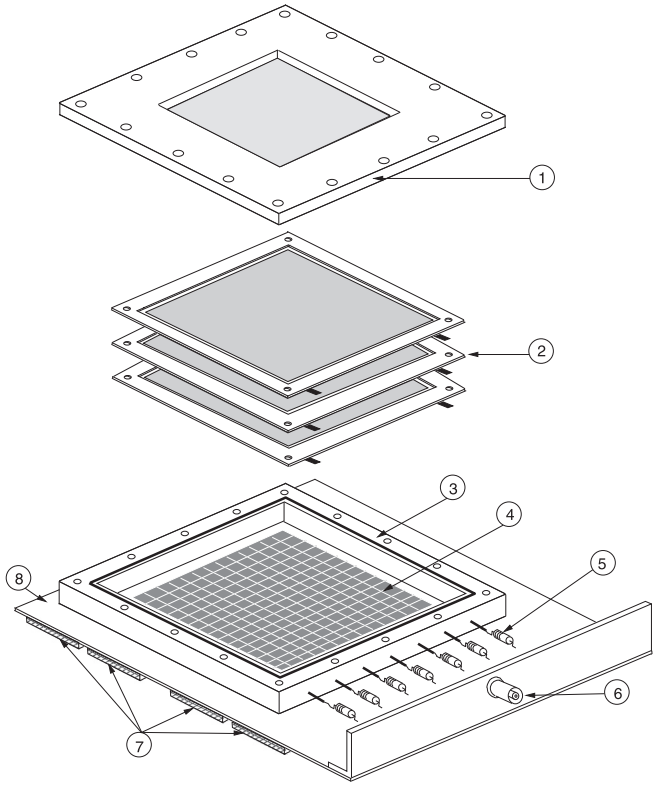

Fig. 3. Schematic of assembly of a triple GEM chamber (1) top chamber lid with drift plane, (2) triple GEM foils stretched in FR4 frames, (3) gas tight housing frame with 'O' ring seal, (4) readout plane, (5) GEM series resistors, (6) SHV connector for bias, (7) input connectors to FEB and (8) readout PCB. The chamber tested at CERN used voltage divider for biasing.

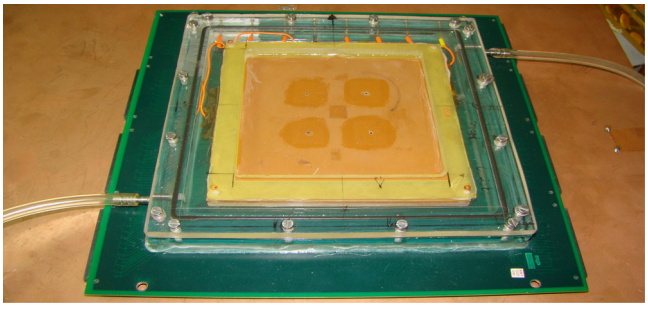

Fig. 4. Photograph of a triple-GEM chamber built at VECC.

channels were applied through a resistive chain and the gas mixture used was Ar–CO_2 in the ratio of 70:30 at atmospheric pressure. The resistive chain is adjusted in such a way that voltages across each GEM were equal.

Another triple-GEM chamber built at GSI-Darmstadt is shown in Fig. 5. This chamber is also made of three CERN-made single mask foils each of dimension 10 cm × 10 cm. The widths of the drift gap, first and second transfer gaps and induction gaps were 3 mm, 2 mm, 2 mm, and 2 mm respectively. The chamber built at GSI was enclosed in a gas tight box of slightly larger volume as compared to the compact design of the VECC chamber. In the GSI chamber, a voltage divider was used to power the GEMs with a protection resistance of 1 MΩ. The readout plane of this chamber had 256 pads each of size 6 mm × 6 mm, traces of which were divided into four connectors. For the results shown in this paper, GSI chamber was at 3.7 kV of total applied voltage and the corresponding drift, transfer and induction fields are 2.19 kV/cm, 3.29 kV/cm and 3.29 kV/cm respectively. In this case, voltages

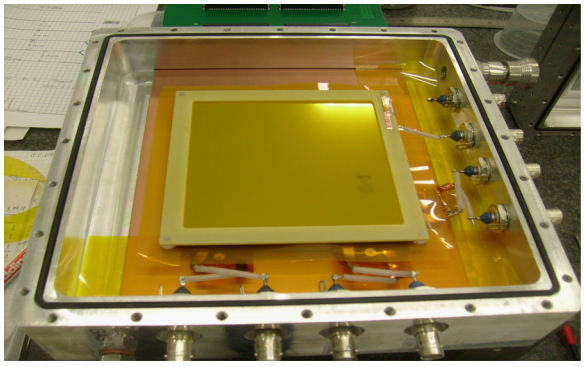

Fig. 5. Photograph of a triple-GEM chamber built at GSI.

Table 1
Parameters of two chambers tested at CERN SPS using pion beams.

Chamber parameters	GEM-1 (mm)	GEM-2 (mm)
Drift gap	3	3
Transfer gap-1	1	2
Transfer gap-2	1	2
Induction gap	1.5	2

across three GEM foils were 370 V, 336 V and 362 V and were not equal for three foils as was the case for VECC-GEM. The gas mixture used was identical to that of the VECC chamber. The parameters of two chambers are summarized in Table 1. In both the chambers, the readout planes covering the central region of the chamber were smaller in the area of varying degree compared to the area of the GEM foil. The areas outside the readout plane were not instrumented.

3. Test beam experimental setup

The layout of the setup used at CERN H4 beam line in October 2012 is shown schematically in Fig. 6. In this testing, pion beams of ≈100 GeV momentum were used. For triggering, two cross-scintillators of 2 cm x 2 cm overlap area placed at the beginning of the setup were put in coincidence with two scintillators of similar dimensions at the end of the setup. The nXYTER-based readout discussed earlier was used in this test run. The coincidence trigger signal was distributed to the ROC auxiliary channels to record the trigger time-stamps.

Two triple GEM chambers built at VECC and GSI are designated as GEM1 and GEM2 respectively in Fig. 6 and have been used in this analysis. In this paper, results on chamber properties are discussed in detail for GEM1 except for some specific results which are shown for GEM2. GEM1 had 512 pads each of 3 mm × 3 mm size read by four FEBs connected to two ROCs. GEM2 had 256 pads each of 6 mm × 6 mm size. GEM2 was read by two FEBs and one ROC. A fiber-optic based readout system was used to minimize the time delay in trigger communication to different ROCs.

In this self-triggered system, all hits above a predetermined threshold as read by nXYTER are digitized and stored, but only the hits produced by beam particles are time-correlated with the trigger. The beam intensity was varied by adjusting the collimator openings which was varied from ±2 mm to ±3 mm. Even though we took data at different beam intensities, for this paper, we have analyzed data taken at rates varying between 400 Hz and 2.5 kHz. We have varied the threshold on nXYTER at different runs, for the results presented here, a threshold corresponding to 1 fC was used.

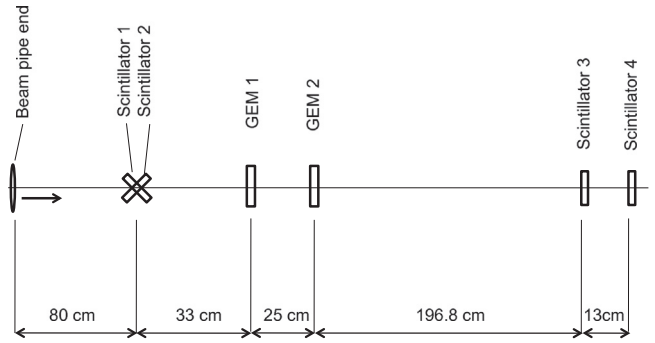

Fig. 6. Test beam setup at the H4 beam line at CERN.

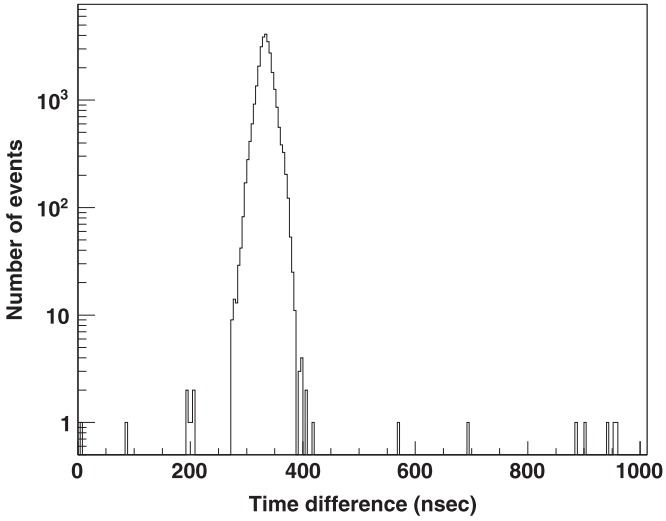

Fig. 7. Distribution of the time difference between the GEM hits and the coincidence trigger. Almost no entries outside the peak show very good noise performance and no uncorrelated hits were found. The Gaussian shape of the correlation peak shows good transfer of charge in the chamber.

4. Results

The first step of data analysis of a self-triggered readout system is to obtain the distribution of time-difference between the time-stamps of the GEM-hits and those of the coincidence trigger signals. Fig. 7 shows the time-difference distribution for a pion run of GEM1 at ΔV_{GEM} of 300 V. The position of the peak depends on the delay introduced by the external delay setting and the cable delay. The distribution shows a well-defined Gaussian shape with a width of 13.5 ns. The fitted-width (σ) of the time-difference spectra varies with the applied voltage as shown in Fig. 8. The fitted width (σ) is related to the time resolution of the chamber which improves with the applied voltage reaching a saturation of $\approx$12 ns at ΔV_{GEM} of 335 V. This result is comparable to the time resolution reported elsewhere [3,10] by triple-GEM chambers of a similar configuration. It should be noted that the actual time resolution would be somewhat better after the subtraction of the time-jitter due to the trigger scintillators. Almost the complete absence of entries on both sides of the time-correlation peak shows that in the current run the chamber had no significant uncorrelated hits.

The GEM-hits inside the time-correlation peaks are considered to be beam-related and the chamber co-ordinates of such hits for GEM1 are plotted in Fig. 9 to show the beam spot at ΔV_{GEM} of 335 V. Given the size of the trigger area, the spread of the spot depends both on the beam-spread and on the size of the electron cluster detected by GEM. The beam spot seen by the detector

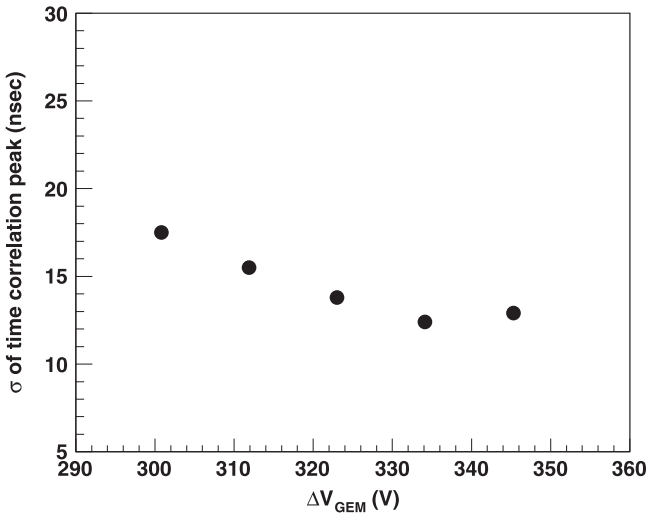

Fig. 8. Variation of σ of the time correlation peak with ΔV_{GEM}. The time resolution of the chamber can be extracted after subtracting the effect of spread introduced by trigger scintillators and the readout electronics. As expected, the time resolution improves with HV.

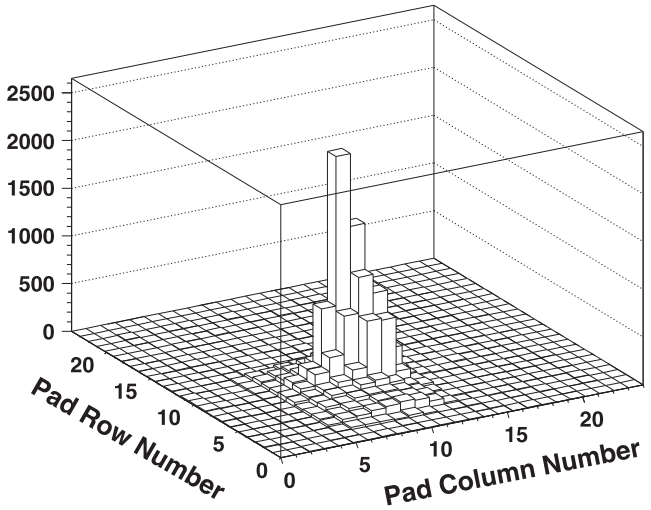

Fig. 9. Pion beam spot on GEM1. This chamber had 3 mm × 3 mm pads.

corresponds to the overlap area of 2 cm × 2 cm of trigger scintillators. However, due to the narrow profile of GEM avalanche spot coupled to the Gaussian shaped beam profile, the beam spot seen on GEM1 is peaked around a few pads only. The beam seems to be narrowly focused and low lying pedestal corresponds to the overlap region of the trigger scintillators. Additionally, uncorrelated noise within the time-correlation window adds hits to the region beyond the trigger area making the spread of the grass wider. For GEM2, operating at higher voltage, the noise is likely to be higher. Fig. 10 shows the beam spot for GEM2. This chamber had 6 mm × 6 mm pads as opposed to 3 mm × 3 mm pads in GEM1. A relatively small number of cells lying outside the peak regions and appear to be correlated to beam are likely to be the result of cross-talks due to the tracks from the cell to the connector. The cross-talk patterns were to be different for the cases of GEM1 and GEM2 as they have different track layouts. The cross-talk pattern will be studied in detail with high intensity beam.

In the next sub-sections, we have discussed various chamber properties like the gain, efficiency, pad-multiplicity and their variations with ΔV_{GEM}. Note that, due to large event statistics in the test run, unless otherwise stated, the statistical errors for all

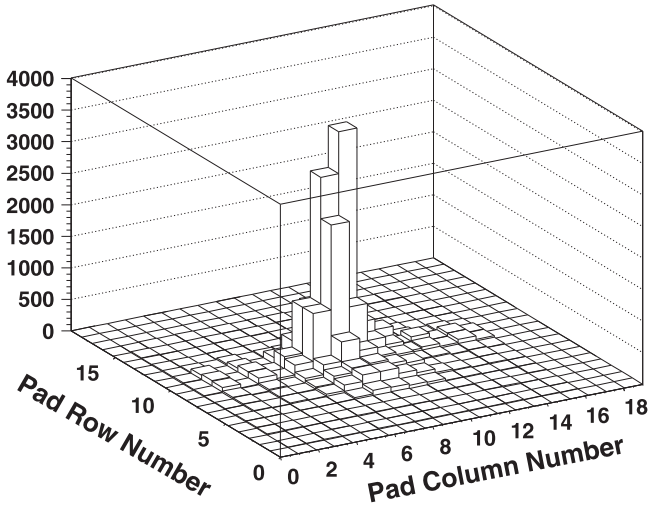

Fig. 10. Pion beam spot on GEM2. This chamber had 6 mm × 6 mm pads.

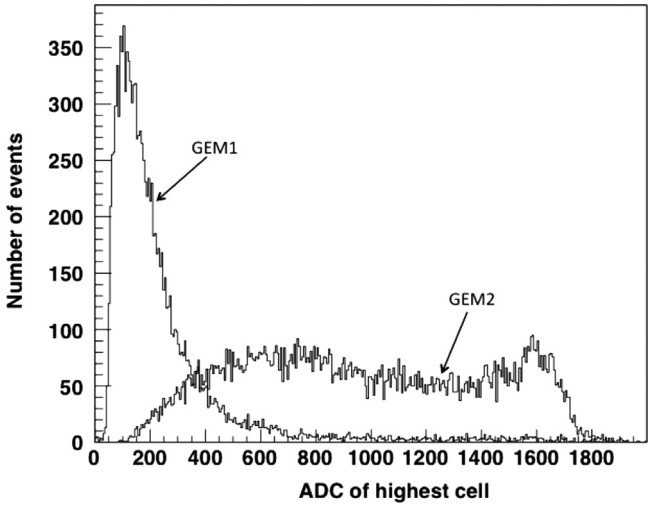

Fig. 11. Spectra of pads with event-wise highest ADC for GEM1 at $\Delta V_{GEM} = 323$ V and of GEM2 at ΔV_{GEM} for three gaps of 370 V, 336 V and 362 V. As expected, a larger fraction of ADC spectra get saturated for GEM2 at this voltage.

the average quantities reported in this section lie within the marker size.

4.1. ADC distribution and gain variation

The pedestal subtracted event-wise highest ADCs are plotted in Fig. 11 for GEM1 at $\Delta V_{GEM} = 323\ V$. A well-defined Landau-shaped distribution characterizing the MIP spectra is seen in the figure. The MIP spectra at different ΔV_{GEM} have been fitted with the Landau function to extract the MPVs of the distributions. At higher ΔV_{GEM}, ADCs show saturation due to a limited dynamic range of nXYTER. In Fig. 11, we have superposed the corresponding ADC distributions for GEM2 at $\Delta V_{total} = 3.7$ kV (corresponding ΔV_{GEM} across three GEM foils are 370 V, 336 V and 362 V) showing a considerably larger fraction of saturating ADC. The chamber-gain has been extracted by adding ADCs of all pads around the maximum in an event. Gains have been extracted only up to $\Delta V_{GEM} = 350$ V beyond which ADC saturates almost completely. We have used the MPV of the MIP spectra at different ΔV_{GEM} for extraction of gain. The errors due to uncertainty in the nXYTER calibration and channel to channel gain variation taken together will be $\approx 16\%$. Fig. 12 shows the variation of extracted gain of

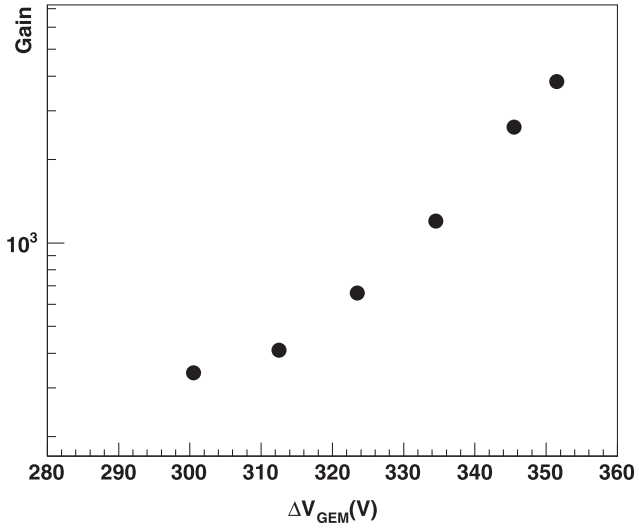

Fig. 12. Variation of gain for GEM1 with ΔV_{GEM}. The gain varies linearly when seen in a log plot.

GEM1 with ΔV_{GEM}. The gain increases slowly at the beginning rising linearly afterwards as shown in Fig. 12. Very slow or no rise at the beginning might be due to nXYTER threshold and incomplete transmission of the electrons through GEM holes. At 350 V, the chamber achieves a gain of ≈ 4000 which is comparable to the gain obtained in Ref. [9]. From the current study, ΔV_{GEM} of 330 V seems to satisfy the criterion of operating voltage. A new ASIC with higher dynamic range is being developed for use in CBM muon chamber use.

4.2. Efficiency

For the operation of CBM-MUCH, attaining an efficiency of $> 95\%$ for MIP is a prerequisite for efficient detection of muons. Additionally, it is required that the efficiency remains stable over the operating range of HV, particle rate and other operating conditions. We have seen earlier that [9] an efficiency of $> 95\%$ is attained with cosmic rays using conventional electronics with a chamber of somewhat larger gap widths. In the test beam experiment reported here, the particles are taken to be detected in an event if there is at least one hit in the time-correlation window. The efficiency is therefore defined as

$$\text{Efficiency} = \frac{N_{GEM}|_{within\ 200\ ns}}{N_{trigger}}$$

where N_{GEM} is the number of events having at least one GEM hit in the time-correlation window and $N_{trigger}$ is the total number of trigger events. We have not made any correction for background as the number of entries outside the peak region is small. This approach might have an overestimation of efficiency by 0.5%.

Fig. 13 shows the variation of efficiency of GEM1 with ΔV_{GEM} for pion data taken in this run. We have shown the results up to the ΔV_{GEM} of 350 V beyond which ADCs are completely saturated due to a limited dynamic range of nXYTER.

A comparison of gain plots in Fig. 12 shows that the efficiency increases till the gain of 10^3 saturating thereafter. An initial increasing trend at $< 90\%$ efficiency in the combined effect of lower gain at those voltages and 1 fC threshold is applied on the nXYTER. In Fig. 11 at ΔV_{GEM} of 323 V, signal and noise are well-separated resulting in a high detection efficiency. From the results shown here, we can conclude that the chamber may be operated at ΔV_{GEM} of 340 V with almost 98% efficiency, i.e., clearly above the required 95% for efficient muon detection.

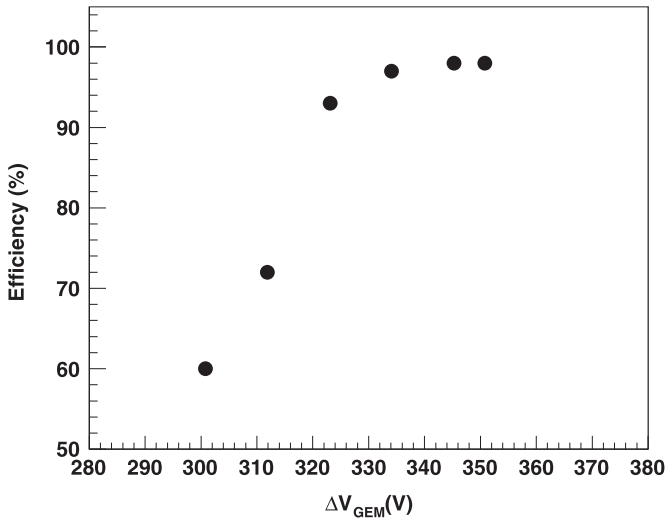

Fig. 13. Variation of efficiency with ΔV_{GEM}. The efficiency increases sharply and reaches a saturation above 95% around ΔV_{GEM} of 335 V.

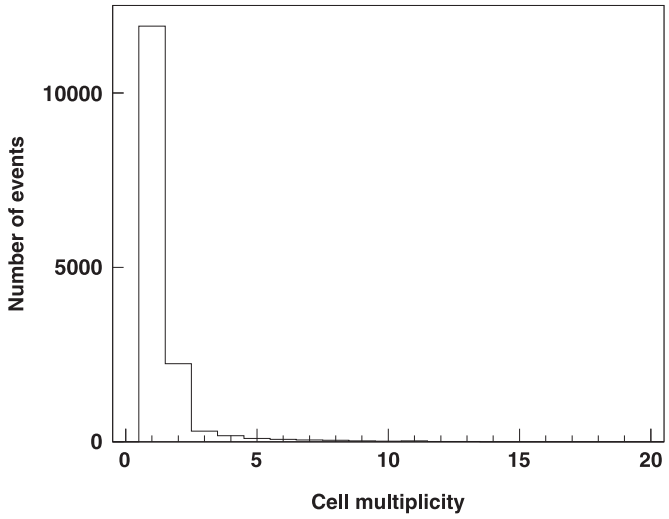

Fig. 14. Distribution of event by event pad multiplicity at $\Delta V_{GEM} = 335$ V. For this chamber of 3 mm × 3 mm pad size, the cluster is confined mostly within one pad.

4.3. Cell multiplicity

As per the literature, the profile of electrons in the GEM detector for comparable detector configuration is expected to cover on an average about three strips of 600 μm width [11]. For a pad-size of 3 mm × 3 mm, it is therefore expected that for the beam particle incident at the middle of the pad, the profile should be confined inside one pad. For projecting tracks on the GEM plane of CBM-MUCH, the cluster size requires detailed study as it determines the particle position. Fig. 14 shows the distribution of pad-multiplicity of GEM1 for a pion run at ΔV_{GEM} of 335 V. The multiplicity has been obtained by taking the time correlated hits located in the trigger region only. The contributions of spatially uncorrelated hits due to noise, contributing up to 10% in pad multiplicity, are therefore reduced. It is seen from Fig. 14 that the hits are confined mostly to one pad. Fig. 15 shows that the average pad multiplicity increases slowly from ≈1.1 at ΔV_{GEM} of 300 V to ≈1.4 at ΔV_{GEM} of 350 V. An increase in gain results in a larger transverse size of the GEM profile which is the likely reason of an increase in pad multiplicity with voltage. The self-triggered noise, which increases with voltage, though low adds to the sources of an increase in pad multiplicity.

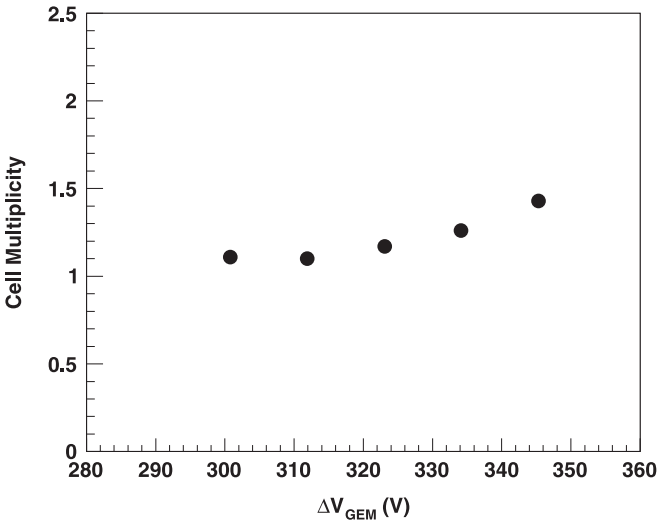

Fig. 15. Variation of average pad multiplicity with ΔV_{GEM}.

5. Summary and discussions

Triple-GEM chambers because of their better spark-rate performance and higher rate handling capabilities among others have been selected by several experiments for muon tracking. Such chambers are being developed to be used as tracking devices in the muon detection system in the CBM experiment at FAIR. Two prototype chambers each made of 10 cm × 10 cm single-mask GEM foils with pad readout and varying granularity have been tested using pion beams at the H4 beam line at SPS-CERN. The detectors have been read by self-triggered ASIC called nXYTER. In this self-triggered system, pad-hits produced by the beam particle are correlated in time with the trigger signal. The width of the time-correlation distribution that is related to the time resolution of the chamber decreases with applied voltage reaching a σ of ≈13 ns at the operating voltage. The time resolution of the chamber demonstrates its capability in resolving hits of 10 MHz rate as required for the muon chambers in the CBM experiment. The chambers operated with Ar–CO_2 gas mixture in 70:30 ratio gives >98% efficiency at $\Delta V_{GEM} = 340$ V. The pad-multiplicity at the operating voltage is ≈1.3 for pion beams. The pad multiplicity increases slowly with voltage suggesting the increase of transverse profile of the chamber. The pad multiplicity close to unity suggests that the position resolution for muon hits will be ≈860 μm as governed by the pad size when divided by $\sqrt{12}$. ADC spectra studied below saturation showed the gain to increase linearly with ΔV_{GEM} reaching ≈4000 at 350 V. An efficiency of >95%, a time resolution of 13 ns and a pad multiplicity of ≈1.3 satisfy the required criteria for CBM-MUCH chambers. The response of the detector to the other set of parameters like rate handling capability, and ageing among others is a matter of further study.

Acknowledgment

We thank T. Nayak of VECC-Kolkata, S. Das, S. Raha, S. Ghosh of Bose Institute, Kolkata, Walter Mueller, P. Senger, S. Linev from GSI-Darmstadt, L. Ropelski and E. Oliveri of RD51 for all helps. We would also like to thank CERN H4 beam line crew for all possible helps. This work is supported by the DAE-SRC award under the scheme no. 2008/21/07-BRNS/2738. Y.P.V. acknowledges the support provided by Helmholtz-Humboldt Research award of Germany and the Raja Ramanna Fellowship of the Department of Atomic Energy, Government of India.

References

[1] F. Sauli, et al., Nuclear Instruments and Methods in Physics Research Section A 386 (1997) 531.
[2] M. Alfonsi, et al., Nuclear Instruments and Methods in Physics Research Section A 581 (2007) 283.
[3] M. Alfonsi, et al., Nuclear Instruments and Methods in Physics Research Section A 518 (2004) 106.
[4] G. Bencivenni, et al., Nuclear Instruments and Methods in Physics Research Section A 488 (2002) 493.
[5] ⟨http://www.gsi.de/forschung/fair_experiments/CBM/index_e.html⟩.
[6] G. Bencivenni, et al., Nuclear Instruments and Methods in Physics Research Section A 494 (2002) 156.
[7] M. Villa, et al., Nuclear Instruments and Methods in Physics Research Section A (2010), doi: http://dx.doi.org/10.1016/j.nima.2010.06.312.
[8] A.S. Brogna, et al., Nuclear Instruments and Methods in Physics Research Section A 568 (2006) 301.
[9] A.K. Dubey, et al., Nuclear Instruments and Methods in Physics Research Section A (2012), doi: http://dx.doi.org/10.1016/j.nima.2012.10.043.
[10] A. Bressan, et al., Nuclear Instruments and Methods in Physics Research Section A 425 (1999) 262.
[11] M. Tytgat et. al., Nuclear Instruments and Methods in Physics Research Section A, http://arXiv:1111.7249v1; F. Simon, et al., arxiv:0711.3751v1.